Chapter 18
Experimental Modal Analysis of a 12 Inch Water Tunnel

Keith Rice, Megan Ewers, Sean Collier, and Nicholas Vlajic

Abstract Water tunnels are one of the most commonly used experimental research facilities for making hydrodynamic measurements of submerged structures. However, because the wave speed of water is close to that of steel, the structural dynamics of the tunnel itself can couple into the water in certain frequency ranges. This fluid-structure coupling may corrupt measurements and lead to errors in instrumentation data during measurements. A modal test was performed on The Pennsylvania State University Applied Research Laboratory's 12 inch (30.5 cm) water tunnel, and compared to acceleration measurements at a number of different flow speeds. These modal results give insights into the observed vibrations of the tunnel while under operation.

Keywords Modal analysis · Fluid-structure coupling · Flow · Measurements · Accelerometers

Introduction

Water tunnel test facilities are the keystone of controlled experimental measurements of structures in a flow field, and are used to characterize the hydrodynamic properties of submerged bodies as well as validate numerical models. The Fluid Dynamics and Acoustics Office at The Pennsylvania State University Applied Research Laboratory maintains and operates four different water tunnels to measure the hydrodynamic properties of submerged bodies in flow fields. The 12 in. (30.5 cm) cross section water tunnel[1] is one of the most widely used water tunnels due to its versatility to support a number of measurements and its cost-effectiveness. A description of the tunnel specifications can be found in Ref. [1], but a short summary is presented here. The water tunnel has two interchangeable test sections that include a circular test section that is 12 in. (30.5 cm) in diameter and 20.0 in. × 4.5 in. (50.8 cm × 11.43 cm) rectangular cross section. The closed-looped variable-speed tunnel can support velocities of 6 ft/s to 69 ft/s (2 m/s to 21 m/s) and pressures of 3 psia to 60 psia (20.7 kPa to 414 kPa), allowing for cavitation studies from cavitation numbers of 0.08 to greater than 350. Additionally, a wire-mesh grid can be inserted into the diffuser of the tunnel that generates turbulent flow within the working section to study the effects of turbulence on bodies. This tunnel has been used to support a number of measurements of two- and three-dimensional bodies such as those of Refs. [2–5].

The tunnel has a number of instrumentation capabilities that include pressure sensors, static and dynamic force gauges, accelerometers, hydrophones and acoustic arrays, and allows for various optical flow measurements. Power spectra data from the different instrumentation and experiments reveal features at common frequencies, leading to speculation that the these features originate from structural resonances of the water tunnel itself. These features are referred to as facility noise and can corrupt measurement signals in certain frequency regimes.

A schematic of the entire tunnel is shown in Figure 1 (left), while a photograph of the rectangular test section is shown in Figure 1 (right).

Keith Rice · Megan Ewers · Sean Collier · Nicholas Vlajic
Applied Research Laboratory, The Pennsylvania State University, University Park, PA, 16802
e-mail: kkr5496@psu.edu; mbe5377@psu.edu; smc604@psu.edu; nav5000@psu.edu

[1] The tunnel is referred to as the 12 in. (30.5 cm) tunnel since the circular cross section is 12 inches (30.5 cm) in diameter. The rectangular cross section, which has a similar area to that of the circular one, was the test section studied here.

Brandon Dilworth et al. (eds.), *Topics in Modal Analysis & Parameter Identification I, Vol. 9*, Conference Proceedings of the Society for Experimental Mechanics Series, https://doi.org/10.13052/97887-438-0154-2_18

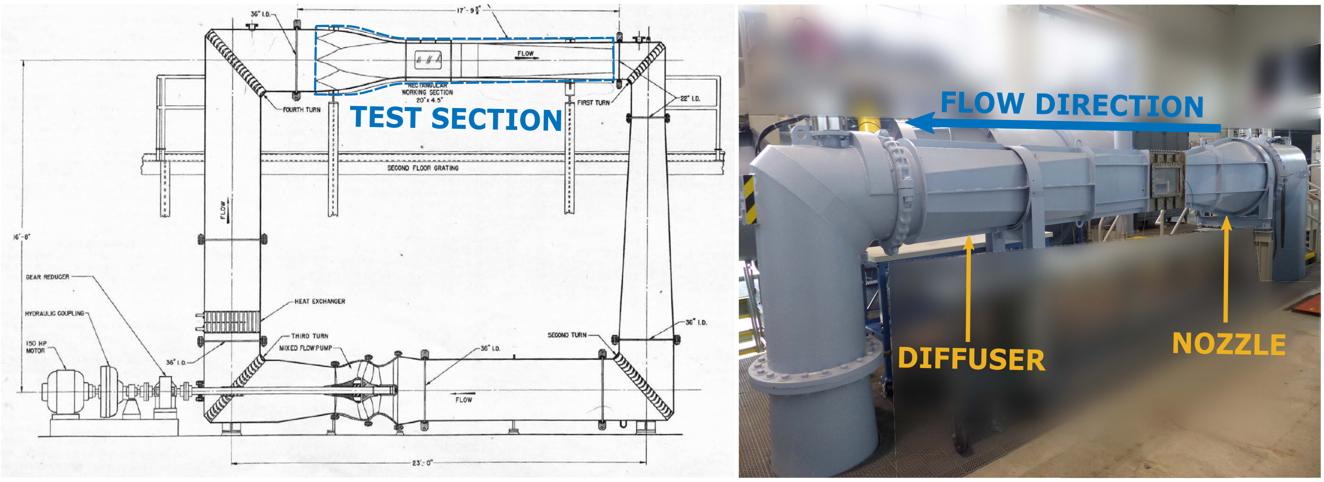

Fig. 1 (Left) Schematic of the entire 12 in. tunnel [1] and (right) photograph of the top portion of the test section that includes the nozzle, working section, and diffuser.

A modal analysis of this tunnel with and without water with the circular test section installed was presented in 2018 [6]. This study showed that the resonant frequencies were reduced by 10% to 15% and the amplitudes of the resonances were reduced up to 15 dB when the tunnel was filled with water. An interesting finding of this study was that the water did not introduce any significant radiation damping into the structure; the attenuated response was primarily due to mass loading. The study focused mostly on the spatial Fourier modes of the structure given its circular geometry. We note that a similar spatial Fourier analysis study is not appropriate for the rectangular cross section studied here given its geometry. For the current study, all data were collected with water in the tunnel.

The intent of this work is to characterize the structural dynamics of the 12 in. (30.5 cm) water tunnel with the rectangular section to gain insights into the origins of the facility noise. Once the nature of this facility noise is better understood, experiments can be designed to avoid certain frequency regimes wherein structural vibrations may be corrupting measurements. Moreover, vibration mitigation strategies can be designed to attenuate some of these undesired structural motions.

Analysis of Vibrations under Operation

Facility noise can originate from a number of different sources, but for the purposes of this study, can be considered as either electrical noise or mechanical noise. Electrical noise includes any electromagnetic interference from electrical utilities, lights, or motors. Mechanical noise can originate from the vibrations of the drive system, including the motor and impeller, as well as fluid-flow forcing on the tunnel itself exciting structural resonances. Initial characterization measurements were made with five accelerometers attached to the tunnel, while operating at six different drive speeds.

Power spectra from one of the accelerometers that highlights the effects of motor drive and structural effects at two different drive speeds are shown in Figure 2. Note that all of the acceleration data reported here were collected without a turbulence grid installed in the diffuser section. Harmonics of the motor at 94.5 RPM (1.58 Hz) (Figure 2 (left)) and 182 RPM (3.03 Hz) (Figure 2 (right)) are marked with numbered dashed lines. It is important to point out that the measured response in Figure 2 is a combination of both the drive amplitude and the structural response, so that the dominant harmonic frequencies may change with drive speed. Although drive speed can be expressed in Hz given some RPM, this is a separate quantity from the drive frequency of the supply phase voltage waveforms which control the drive speed.

In the 94.5 RPM data shown in Figure 2 (left), harmonics 5 and 7 are particularly notable, since they are likely excited by the three phases in the motor ($3\times2 \pm 1$) [7]. At 94.5 RPM, harmonics 5 and 7 are near 8 Hz and 11 Hz, respectively. At 182 RPM shown in Figure 2 (right), harmonics 5 and 7 are still present, but the 7th harmonic is not as strong. There is still a response in spectra near 8 Hz and 11 Hz at 182 RPM, which are likely resonant modes of the structure. At lower frequencies, when the harmonics of the drive system align with these resonances, there is an amplified response.

Power spectra from the same accelerometer as Figure 2 at six different flow speeds are shown in Figure 3. Low frequency spectra (under 50 Hz for this study) are shown in Figure 3 (left), while the broadband response (up to 1 kHz) is provided in Figure 3 (right). All data were collected with 100 second durations, sampling at 20.48 kHz. The low-frequency power spectra

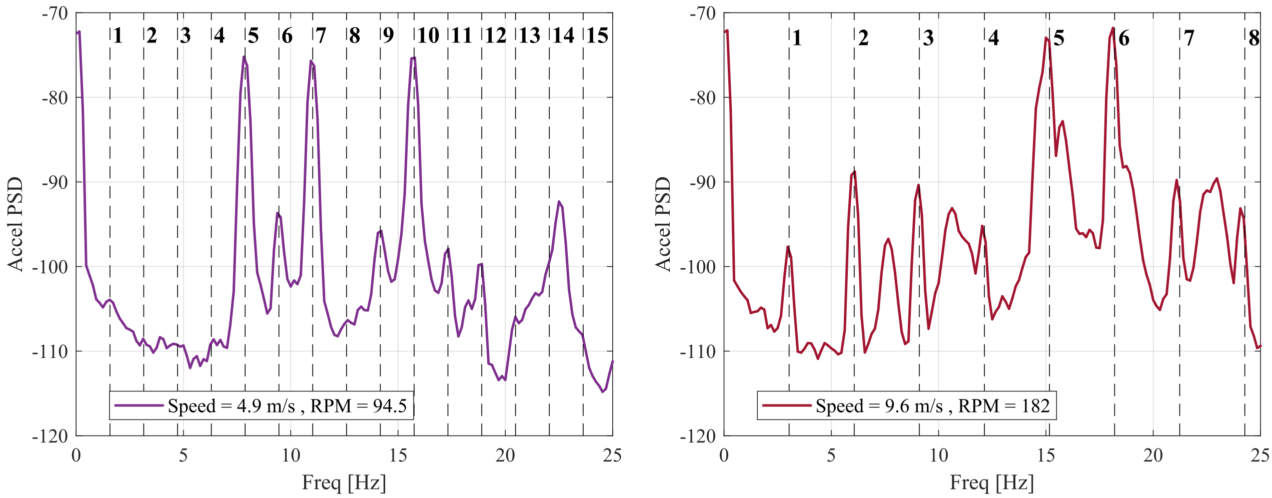

Fig. 2 Acceleration spectrum of an accelerometer mounted on the outside of the tunnel while the motor was operating at 94.5 RPM (1.58 Hz) (left) and 182 RPM (3.03 Hz) (right). Harmonics of the drive speed are shown as vertical dashed lines.

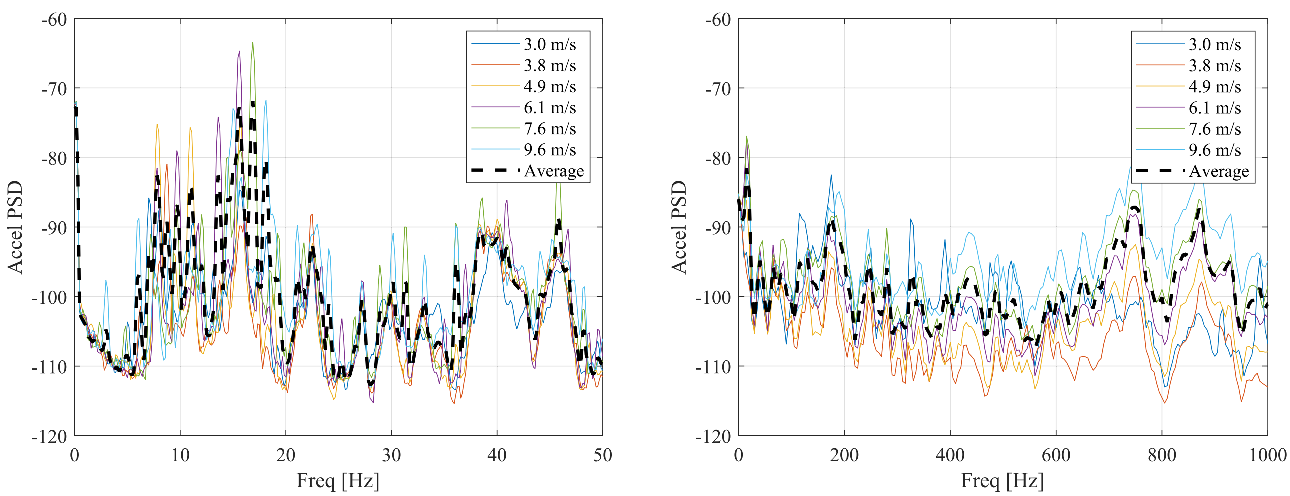

Fig. 3 Low (left) and high (right) frequency regimes of acceleration spectra at different operating speeds.

were calculated using 25 averages with 25% overlap, while the high-frequency data were calculated using 500 averages with 25% overlap.

When looking at the response spectra of the accelerometer, structural resonances excited by flow-induced forcing will not change with drive speed since the forcing is broadband. However, driving excitation from the motor and impeller are expected to generate tonal forcing that change with drive speed, even though the resonances will be unchanged.

As a first approximation to remove the tonal effects of the motor drive from the structural response, the amplitude spectra were averaged over all the drive speeds and the result is shown in a dashed black line.

When looking at the averaged response in the low frequency data (shown in Figure 3 (left)), prominent features in spectra occur at 7.8 Hz, 8.8 Hz, 10.9 Hz, 13.6 Hz, 15.6 Hz, 16.9 Hz, 18.1 Hz, with the two highest amplitude spectra being 15.6 Hz and 16.9 Hz. Note that although these results are averaged spectra, the individual spectra at each drive speed tend to vary around these frequencies. The spectral response between 25 Hz and 50 Hz tend to be more constant with respect to drive speed, indicating that excitation in this regime is likely from flow-induced forcing. The broadband data (shown in Figure 3 (right)) tend to have frequency components that do not change with flow speed, although the amplitude generally increase with flow speed above 600 Hz.

Experimental Modal Analysis

Due to the size of the structure and the nature of the anticipated modes, a roving hammer modal analysis was performed on the test section of the tunnel. Six single-axis accelerometers were affixed to the tunnel in three orientations which aligned with Cartesian axes as shown in Figure 4. This set of accelerometers contained the same accelerometers that were used in the drive speed testing and were thus at the same locations. The tunnel was filled with non-flowing water to account for fluid-structure coupling. Two tests were done separately, namely, a “low-frequency” test and a “high-frequency” test. The intent of the “low-frequency” test was to excite modes below 100 Hz. A 2.4 lb (1.1 kg) PCB Piezotronics 086D20 hammer was used to hit 114 points that were coarsely spaced since these modes of the tunnel will have low wave-numbers.

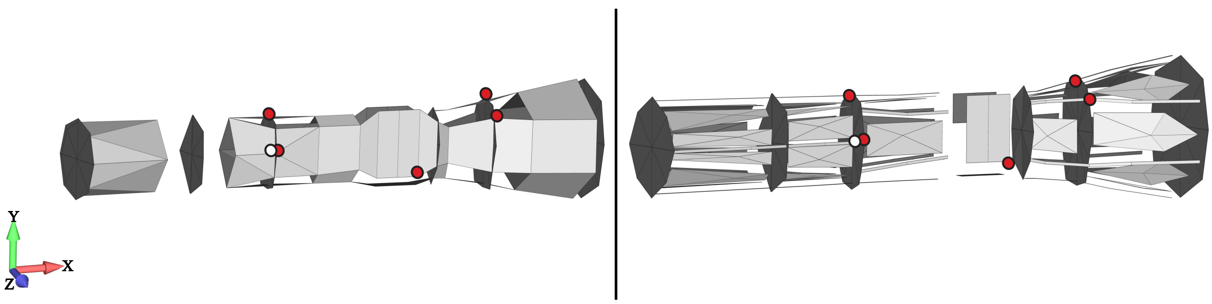

Fig. 4 Low-frequency (left) and high-frequency (right) experimental meshes with accelerometer locations marked. White dots were used to improve the visibility of two locations in close proximity.

For the “high-frequency” test a 0.7 lb (0.32 kg) PCB Piezotronics 086D05 hammer with a metal tip was used to excite the structure to identify modes up to at least 1 kHz. For this high-frequency test, the finer mesh consisting of 335 hit locations (including the 114 from the low-frequency test) was used to resolve the motion since the wave numbers are larger at the higher frequencies.

Each strike was performed three times to achieve an average spectrum. Note that accelerometers and hit points were only place along the test section and not the entire tunnel itself (see Figure 1 (left)). Care must be taken when analyzing results, especially any modal assurance criteria, since there may appear to be spatial aliasing as the entire tunnel was not instrumented.

The meshes were constructed using elements that had surface normal vectors that matched the direction of the surface being struck in order to move along the same vectors as the accelerometer data; faces of the tunnel that were not struck were omitted from the meshes because there was no data to reliably describe their movement.

The PolyMAX algorithm was used to identify modes from the data [8]. A mode order of 26 was used for the low-frequency test, searching from 0 Hz to 100 Hz. A mode order of 40 was used in the high-frequency test, searching between 100 Hz and 300 Hz. The identified modes were then cross-referenced with the experimental acceleration spectra from the drive speed testing in Figure 3 to identify modes that may be excited during normal tunnel operation.

Results

A comparison between the normalized surface average mobility from the modal test and the average acceleration of the operational drive-speed test at low frequencies is shown in Figure 5. The operational test trace has correlation with the modal test trace at several frequencies, most notably near 15 Hz.

Modes pertinent to both the surface averaged acceleration from the modal test and the drive speed accelerometer data are depicted on the following pages in Figures 6 and 7.

The low-frequency data contains modes at 7 Hz, 8 Hz, and 10 Hz, along the z-, x-, and z-axes respectively. Some of these low-frequency modes look like modes with free or fixed ends but in fact include motion of the rest of the tunnel. While the test section was sufficiently spatially resolved, there was modal participation from the lower sections of the tunnel which was not resolved. The tunnel has an unusual shape, namely, a cross-section that transitions from a circle to rectangle to circle with a decreasing and increasing effective area. Despite this atypical geometry, some of the lower order modes are representative of bending motions of a beam. The first bending mode on the z-axis (about the y-axis) occurs at 15 Hz. The first bending mode on the diagonal between the y- and z-axes occurs at 27 Hz, while 37 Hz represents the first bending mode on the y-axis but second on the z-axis.

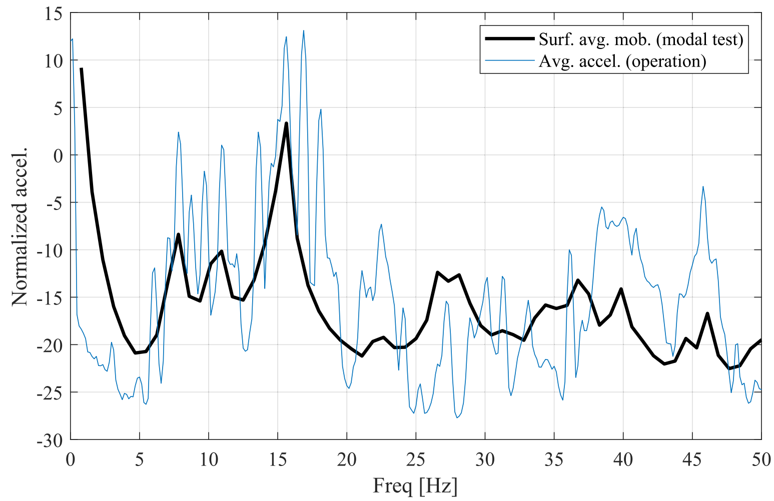

Fig. 5 Comparison of operational accelerometer data with low-frequency modal surface average accelerance data.

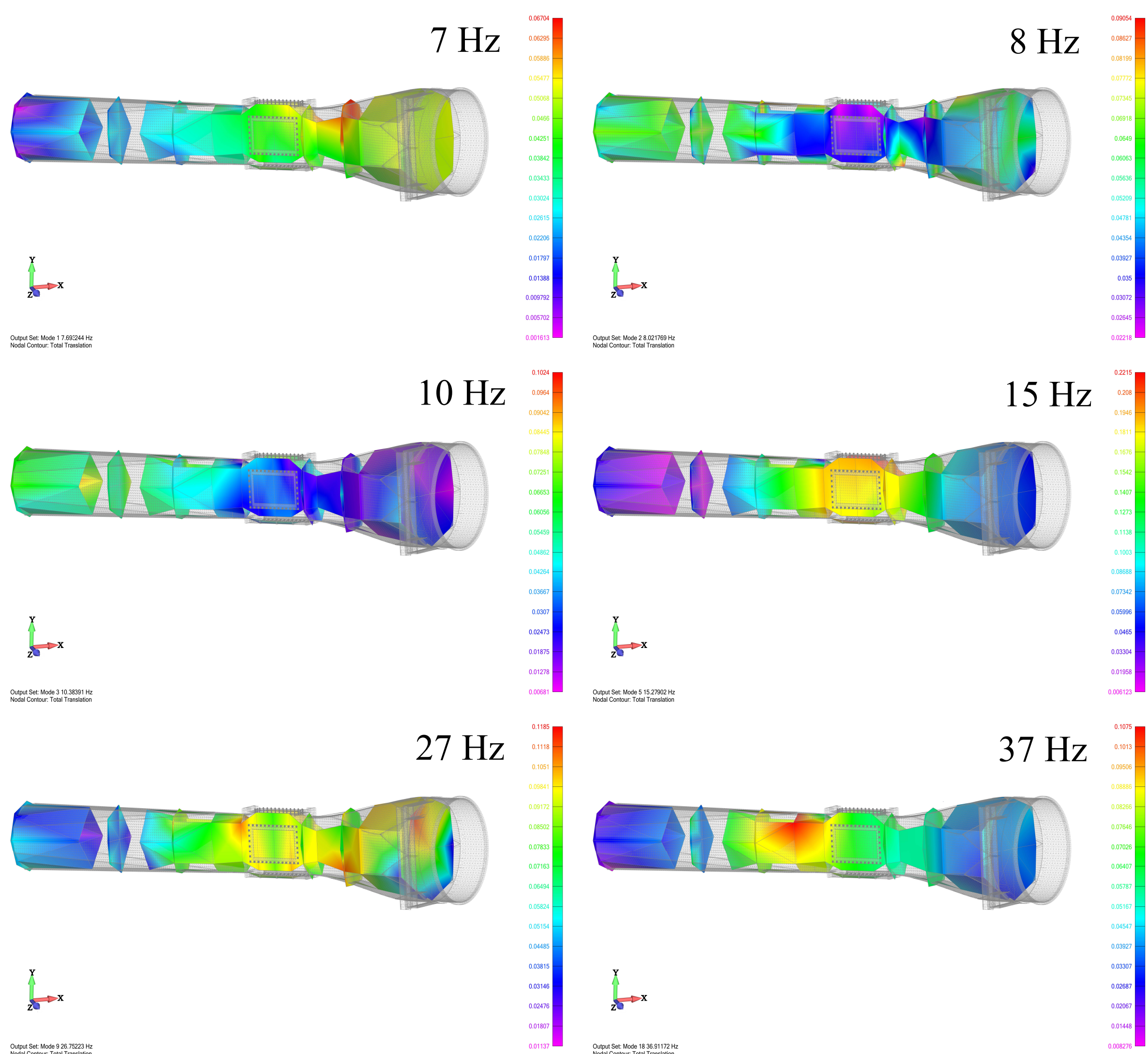

Fig. 6 Modes of interest below 50 Hz that correspond to higher amplitude regimes of operational acceleration data.

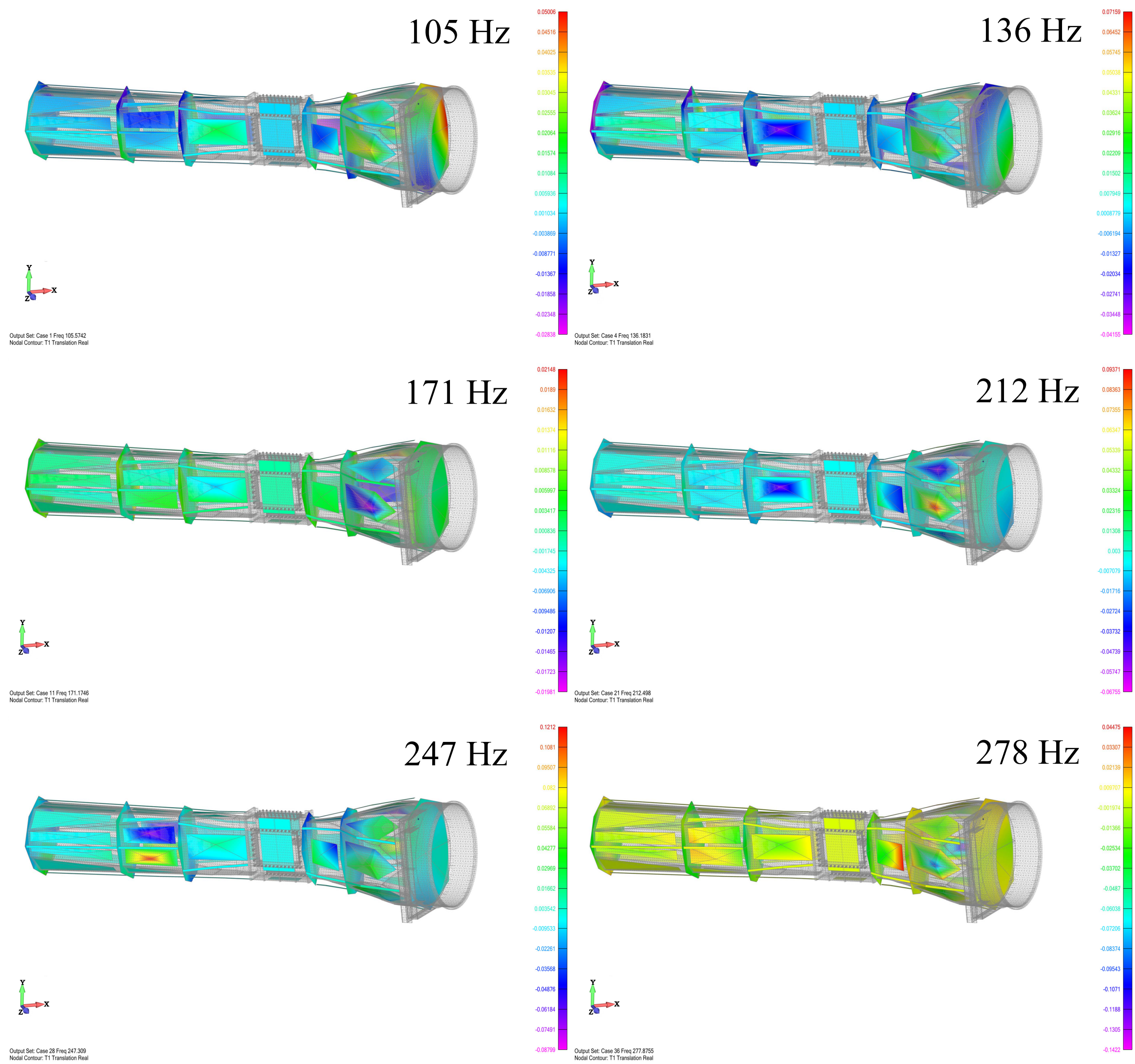

Fig. 7 Modes of interest above 100 Hz that correspond to higher amplitude regimes of operational acceleration data.

The identified high-frequency modes are documented in Figure 7. The modes in Figure 7 indicate tunnel vibrations nearest the following peak frequencies from the data in Figure 3: 100 Hz, 130 Hz, 175 Hz, 210 Hz, 245 Hz, and 280 Hz.

In this higher frequency regime, the modes don't necessarily behave as simple beam-bending modes and the motion becomes more complex. Not every peak in the operational acceleration data was reflected in the modal data, and vice versa. At higher frequencies, the system becomes modally dense and discerning real modes becomes difficult.

As noted earlier, the operational data in Figure 3 was taken without a turbulence grid installed. In conditions wherein the turbulence grid is installed, turbulent flow through the tunnel is expected to excite these high-frequency modes and create an amplified response in the accelerometer readings over a large bandwidth.

Discussion and Conclusion

The results presented here are useful for interpreting past data collected in this facility, as well as future tests. Acceleration spectra during tunnel operation contains both broadband characteristics, and tonal features from both the motor drive and structural resonances of the tunnel. The modal analysis performed on the tunnel showed that the the structural response of the tunnel is modally dense, due to the size of the tunnel and of the fluid-structure interaction. Errors in instrumentation located within the tunnel can be amplified when harmonics of the motor drive speed align with structural resonances of the tunnel at the lower frequencies, below 100 Hz. At higher frequencies, above 100 Hz, other resonances were observed and are assumed to be excited by fluid flow forcing through the tunnel. However, the acceleration spectra during operation is complex in nature and the presence of a strong response at a particular frequency in experimental acceleration data may not imply an excited vibration mode; similarly, an existing structural mode may not be excited during the course of an experiment. The data collected here did not have the wire-mesh turbulence grid inserted into the diffuser. The presence of this grid is expected to exacerbate the fluid flow forcing and introduce additional tonal features from resonances of the grid itself. Further analysis with and without the turbulence grid may yield additional insights. For example, asynchronous and synchronous averaging, as well as instrumenting the motor and performing coherent noise rejection may also reveal additional information to the nature of the spectral response of the tunnel.

Acknowledgments The authors would like to acknowledge Hruday Shah, Victor Baran, and Sierra Nelson for their assistance with the experiments.

References

1. Lehman, A.F. "The Garfield Thomas Water Tunnel". In *Bodarski Institut, Shipbuilding Research Institute Zagreb, Presented at: The Symposium on the Towing Tank Facilities, Instrumentation and Measuring Technique, 22-25 September 1959* (1959).
2. Stinebring, D.R., Straka, W.A., and Willits, S.M. "Hydrofoil test facility at ARL Penn State". In *Fluids Engineering Division Summer Meeting*, volume 41995, pages 603–607 (2005).
3. Reich, D.B. *Water tunnel experiments on a model scale helicopter rotor hub*. M.S. Thesis, The Pennsylvania State University (2013).
4. Brungart, T.A., Myer, E.C., Capone, D.E., and Campbell, R.L. "Hydrofoil vibration and noise reduction with leading edge isolation". In *INTER-NOISE and NOISE-CON Congress and Conference Proceedings*, volume 2005, pages 623–629. Institute of Noise Control Engineering (2005).
5. Lysak, P.D., Capone, D.E., and Jonson, M.L. "Measurement of the unsteady lift of thick airfoils in incompressible turbulent flow". *Journal of Fluids and Structures*, 66:315–330 (2016).
6. Myer, E., Bonness, W., and Fahnline, J. "Modal analysis results of ARL/PSU 12" water tunnel test section with and without water". In *Intenational Modal Analysis Conference XXXVI, Orlando, FL* (2018).
7. Gieras, J.F., Wang, C., and Lai, J.C. *Noise of polyphase electric motors*. CRC press (2018).
8. Guillaume, P., Verboven, P., Vanlanduit, S., Van Der Auweraer, H., and Peeters, B. "A poly-reference implementation of the least-squares complex frequency-domain estimator". In *Proceedings of IMAC*, volume 21. A Conference & Exposition on Structural Dynamics, Society for Experimental Mechanics (2003).